RSC Advances

PAPER

View Article Online
View Journal | View Issue

Cite this: *RSC Adv.*, 2022, **12**, 22210

Polydiacetylene-based colorimetric and fluorometric sensors for lead ion recognition†

Shu-Wei Chen, * Xipeng Chen, Yang Li, Yalin Yang, Yuchuan Dong, Jinwen Guo and Jinyi Wang *

Development of novel sensors for the detection of lead ions (Pb^{2+}) has attracted increasing interest due to their inherent toxic effects on human health and the environment. In this study, we describe two new polydiacetylene (PDA)-based liposome sensors for the colorimetric and fluorometric recognition of Pb^{2+} in aqueous solution. In the sensor system, a thymine-1-acetic acid (TAA) or orotic acid (OA) group was reasonably introduced into the diacetylene monomer to work as a strong binding site for Pb^{2+}. The TAA- or OA-functionalized monomer and 10,12-pentacosadiynoic acid (PCDA) were incorporated into PDA liposomes in aqueous solution. After UV light-induced polymerization, deep blue colored liposome solutions were obtained. Upon the addition of a series of transition metal cations into the liposome solutions, only Pb^{2+} could induce a color change from blue to red observable by the naked eye and a large fluorescence enhancement. The results clearly showed that the PDA–EDEA–TAA and PDA–EDEA–OA liposomes could act as highly selective and sensitive probes to detect Pb^{2+} in aqueous solution. The detection limits of PDA–EDEA–TAA and PDA–EDEA–OA systems are 38 nM and 25 nM, respectively. The excellent selectivity of PDA liposomes could be attributed to the stronger complexation behavior of Pb^{2+} with TAA (or OA) and the carboxylic acid at the lipid–solution interface which could perturb the PDA conjugated backbone. In addition, the proposed sensors were successfully applied to detect trace amounts of Pb^{2+} in real water samples with excellent recovery, indicating that the developed method had a good accuracy and precision for the analysis of trace Pb^{2+} in practical samples.

Received 2nd June 2022
Accepted 5th August 2022

DOI: 10.1039/d2ra03435b

rsc.li/rsc-advances

1 Introduction

Environmental pollutants such as heavy metals have had a dramatic impact on ecosystems over the past few centuries. Among the various heavy metal ions, lead ions (Pb^{2+}) in particular remain one of the most important targets, and have inherent toxic effects on human health and the environment.[1] It is reported that even a very small amount of Pb^{2+} exposure can cause memory loss, muscle paralysis, anemia and intellectual disability.[2,3] However, lead can be easily encountered in the environment due to its use in gasoline, batteries, pigments, *etc.* In 2011, the World Health Organization established guidelines for drinking water quality with a provisional guideline value of 10 μg L^{-1}.[4] At present, the most typical detection methods of trace Pb^{2+} are mainly focused on the atomic absorption spectroscopy, inductively coupled plasma mass spectrometry and electrochemical techniques.[5–7] These traditional methods can be used to analyze the total content of Pb^{2+} with high sensitivity. However, the requirements of expensive cumbersome instruments, extensive pretreatment of samples and skilled professionals limit their application for rapid detection and *in situ* analysis.[8] To overcome the above limitations, quite a number of fluorescent chemosensors based on DNAzyme,[9–13] proteins,[14] polymers,[15] nanoparticles,[16–19] peptides[20] and small molecules[21–25] have been developed for Pb^{2+} detection over the last few decades. Although some of the sensors such as DNAzyme-, protein-, and peptide-based sensors displayed high sensitivity and selectivity in aqueous solutions, their complicated process and relative instability always prevent their practical applications.[24] Therefore, the development of sensitive and convenient methods for Pb^{2+} detection in aqueous solution is still a challenge and of great interest.

Polydiacetylenes (PDAs), a representative class of conjugated polymers, have been extensively investigated and utilized as intriguing materials for sensing applications due to their sensitive colorimetric/fluorescent dual detection capabilities.[25,26] Diacetylene monomers can easily self-assemble in an aqueous medium to form liposomal structures that can be photopolymerized to generate PDA with a blue color (absorption λ_{max} at 640 nm).[27] Upon exposure to external stimuli, the absorption λ_{max} of PDA shifts from 640 nm (blue phase) to 540 nm (red phase). Interestingly, the triggered red phase of PDA is also weakly fluorescent, so PDA can provide dual

College of Chemistry & Pharmacy, Northwest A&F University, Yangling, Shaanxi 712100, P. R. China. E-mail: chenshuwei2011@nwsuaf.edu.cn; jywang@nwsuaf.edu.cn

† Electronic supplementary information (ESI) available. See https://doi.org/10.1039/d2ra03435b

signaling capability. The stimulus-induced intense blue-to-red transition and fluorescence enhancement of the PDAs have led to the development of various chemosensors.[28] The dual signal generation is mainly attributed to the interfacial perturbation of PDAs caused by external stimuli, which can subsequently induce a conformational change of the PDA conjugated backbone. To date, a variety of PDA-based sensors have been developed for chemical, biological and environmental analytes such as virus,[29] DNAs,[30] enzymes,[31–35] proteins,[36,37] metal ions,[38–41] surfactants[42–44] and organic solvents.[45,46] In addition, a few examples of PDA-based colorimetric sensors for Pb^{2+} detection have also been reported (Fig. 1).[47–53] Certainly, naked-eye detection is the simplest process that can be applied for environmental purposes.

With the aim to develop more efficient PDA-based sensors for Pb^{2+} recognition, herein we first designed and synthesized thymine-1-acetic acid- and orotic acid-functionalized diacetylene monomers PCDA–EDEA–TAA and PCDA–EDEA–OA since the carbonyl group in thymine-1-acetic acid or orotic acid possesses high complexing power toward Pb^{2+} (Scheme 1).[54] The binding constants of PDA–EDEA–TAA for various metal ions were calculated according to previously reported methods and shown in Table S1.†[55,56] By co-assembly of PCDA–EDEA–TAA (or PCDA–EDEA–OA) and 10,12-pentacosadiynoic acid (PCDA), two new PDA-based liposome chemosensors for colorimetric and fluorometric detection of Pb^{2+} were obtained. Upon the addition of various metal ions into the liposome solutions, only Pb^{2+}

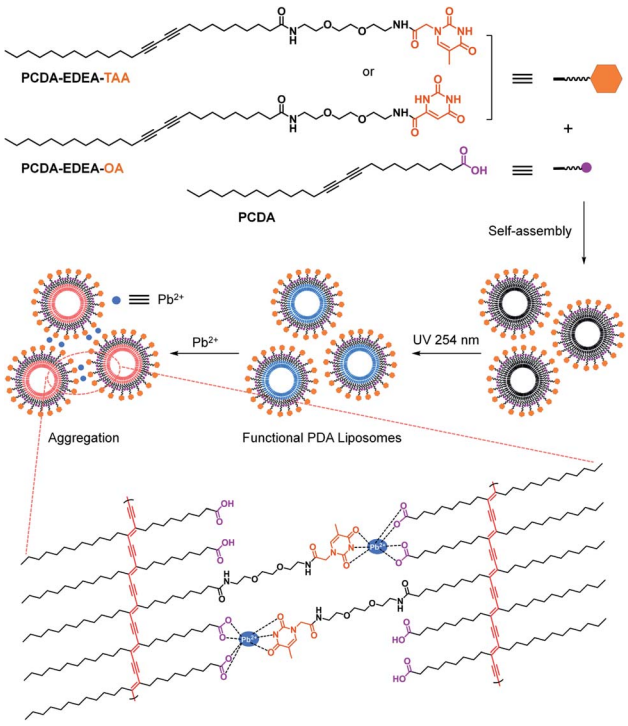

Scheme 1 Schematic illustration of the formation and aggregation of functional PDA vesicles.

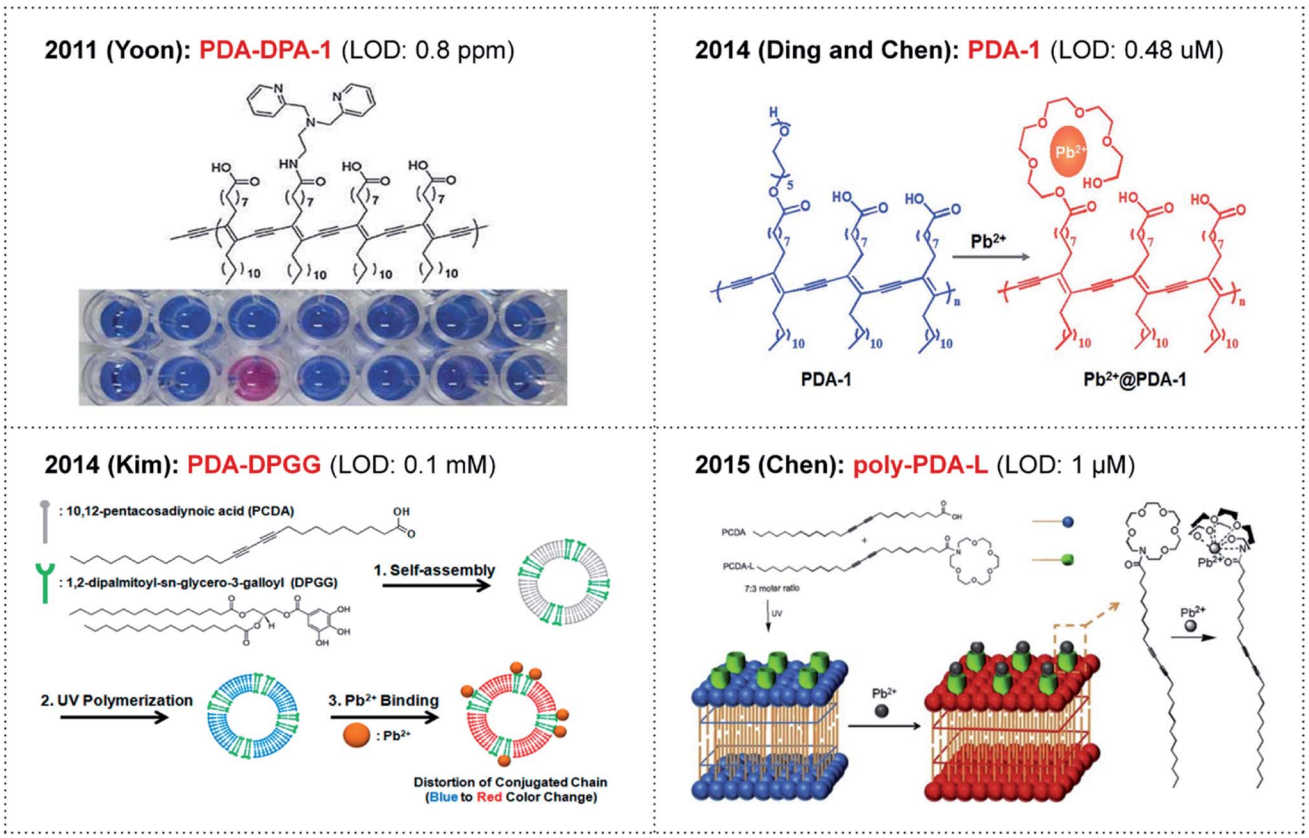

Fig. 1 Representative PDA-based colorimetric sensors for Pb^{2+} detection.

could cause a distinct color change from blue to red observable by naked eye and a dramatic fluorescence enhancement, which clearly showed that PDA–EDEA–TAA and PDA–EDEA–OA liposomes possessed excellent selectivity and high sensitivity. The current work may offer new method for Pb^{2+} recognition in a more efficient manner.

2 Results and discussion

2.1 Optimization of PDA liposome components

To obtain effective PDA liposome sensors for Pb^{2+} detection, it is desirable to investigate the optimal PDA liposome components since the monomer compositions in the liposome can significantly affect its recognition and sensing behavior.[57] A series of PDA liposome solutions were prepared by using different mole ratios of PCDA–EDEA–TAA (or PCDA–EDEA–OA) and PCDA. After photoinduced polymerization under 254 nm UV light, blue colored suspensions were obtained. The colorimetric responses of each kind of PDA liposomes in the presence of different concentrations of Pb^{2+} were then examined (Fig. 2). It can be seen that PDA liposomes prepared from PCDA–EDEA–TAA (or PCDA–EDEA–OA) and PCDA with different mole ratios displayed different color responses to Pb^{2+}. Among them, PDA liposomes prepared with a 1 : 9 mole ratio of PCDA–EDEA–TAA (or PCDA–EDEA–OA) and PCDA showed the most distinct color changes from blue to red in the presence of 100 μM Pb^{2+} (Fig. 2a and b). Color changes of PDA liposomes prepared from PCDA–EDEA–TAA and PCDA (mole ratio, 1 : 9) became more apparent with the increased concentrations of Pb^{2+} (0–100 μM) (Fig. 2c). A discernible color change from blue to purple was observed when 20 μM of Pb^{2+} was added, indicating the potential application of PDA liposomes for Pb^{2+} recognition in the naked-eye. The colorimetric response values (CR, %) calculated using the UV-vis absorbance spectroscopic data were about 60% (PCDA–EDEA–TAA) and 52% (PCDA–EDEA–OA) when 100 μM Pb^{2+} was added respectively (Fig. 3). With the increase of the monomer component PCDA–EDEA–TAA (or PCDA–EDEA–OA) in the liposomes, the color responses of PDA liposomes to Pb^{2+} gradually decreased. When the mole ratio of PCDA–EDEA–TAA (or PCDA–EDEA–OA) to PCDA reached 5 : 5, the PDA liposomes exhibited little color change, even after 100 μM of Pb^{2+} was added (CR, ~4%). PDA liposomes derived from pure PCDA was also investigated and slight color changes were displayed (CR, ~5%). These results demonstrate that both the carboxylic acid groups and thymine-1-acetic acid (or orotic acid) groups are essential for the colorimetric detection of Pb^{2+}, and the mole ratio of carboxyl acid group to thymine-1-acetic acid (or orotic acid) group on the surface of PDA liposomes plays a key role in the recognition of Pb^{2+}. It is desirable to note that a suitable local "micro-environment" produced by the two groups is important for the detection of Pb^{2+}.[57] In view of the color change results, PDA liposomes prepared from 1 : 9 mole ratio of PCDA–EDEA–

Fig. 2 Color changes of PDA liposomes prepared from (a) PCDA–EDEA–TAA and PCDA, (b) PCDA–EDEA–OA and PCDA in different mole ratios (5 : 5, 4 : 6, 3 : 7, 2 : 8, 1 : 9, 0 : 10) before and after the addition of 100 μM Pb^{2+}. (c) Color changes of PDA liposomes prepared from PCDA–EDEA–TAA and PCDA (1 : 9) in the presence of different concentrations of Pb^{2+} (0, 5, 10, 15, 20, 25, 30, 40, 50, 60, 70, 80, 100 μM).

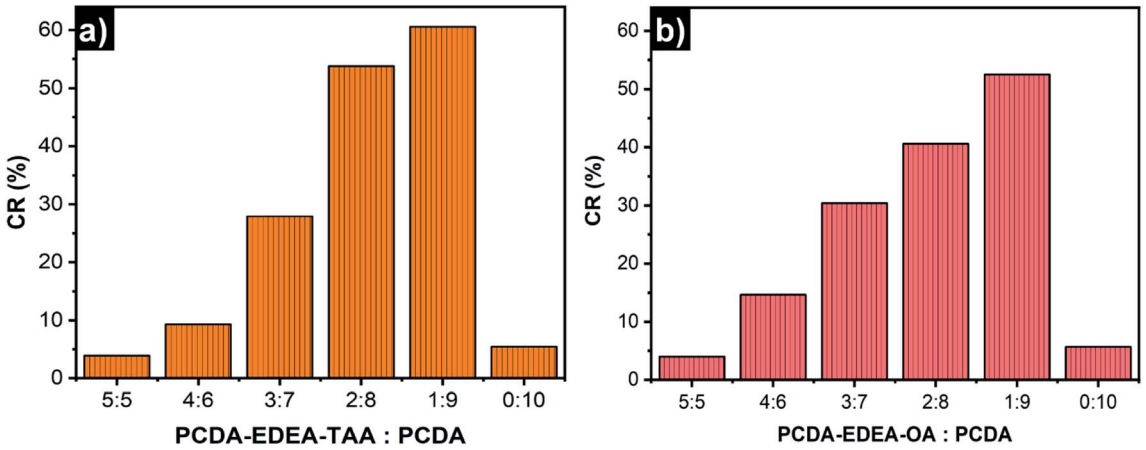

Fig. 3 CR (%) values of PDA liposomes (100 μM) prepared from different mole ratios of (a) PCDA–EDEA–TAA and PCDA, (b) PCDA–EDEA–OA and PCDA in the presence of 100 μM Pb^{2+} ions.

TAA (or PCDA–EDEA–OA) to PCDA (denoted as PDA–EDEA–TAA or PDA–EDEA–OA) was chosen as the optimal detection system for further investigation on Pb^{2+} detection.

2.2 The mechanism of PDA liposomes for Pb^{2+}

To gain insight into the detection mechanism of PDA–EDEA–TAA liposomes for Pb^{2+}, the size changes of PDA–EDEA–TAA liposomes were investigated by using the dynamic light scattering (DLS) method.[57,58] Prior to being irradiated with UV light, the liposome particles exhibited an average size of 122 nm (Fig. S4a†). The size of the liposome contracted to 91 nm after 254 nm UV light treatment because the polymerization of the diacetylene monomers could make the lipid molecules compact (Fig. S4b†). The size of PDA–EDEA–TAA liposomes increased to 955 nm in the presence of 100 μM Pb^{2+} (Fig. S4c†). Morphological studies by using the transmission electron microscopy (TEM) also showed that only Pb^{2+} or PDA–EDEA–TAA liposomes were almost spherical and well separated (Fig. 4a and b). However, the addition of 100 μM Pb^{2+} induced extensive aggregation of liposomes (Fig. 4c). These phenomena confirmed the strong complexation of Pb^{2+} with both carboxyl group and thymine-1-acetic acid groups, which further resulted in the aggregation of PDA–EDEA–TAA liposomes. These intermolecular and intramolecular interactions were believed to produce the interfacial perturbations of the PDA and subsequently resulted in the conformational changes of PDA conjugated backbone. The resulting color change and fluorescence transition can be used for naked-eye detection of Pb^{2+}.

An *in situ* ^{1}H-NMR spectroscopy was also performed to further verify the intense complexation of Pb^{2+} with carboxyl and thymine-1-acetic acid groups. As shown in Fig. S5,† the bottom blue NMR spectrum was a mixture of PCDA and PCDA–EDEA–TAA in a 9 : 1 mole ratio, and the peaks at 11.97 and 11.27 ppm were the characteristic resonance signals of –COO*H* and –N*H*–, respectively. The top red NMR spectrum was the mixture after adding 100 μM Pb^{2+} for 5 min. As can be seen from the spectra, the resonances of the –COO*H* and –N*H*– protons were easily observed before the addition of Pb^{2+}. However, after the addition of Pb^{2+} for 5 min, the resonance peaks at 11.97 and 11.27 ppm were completely disappeared. All the above results demonstrated that Pb^{2+} could form complexes with carboxyl and thymine-1-acetic acid groups, as depicted in Scheme 1.

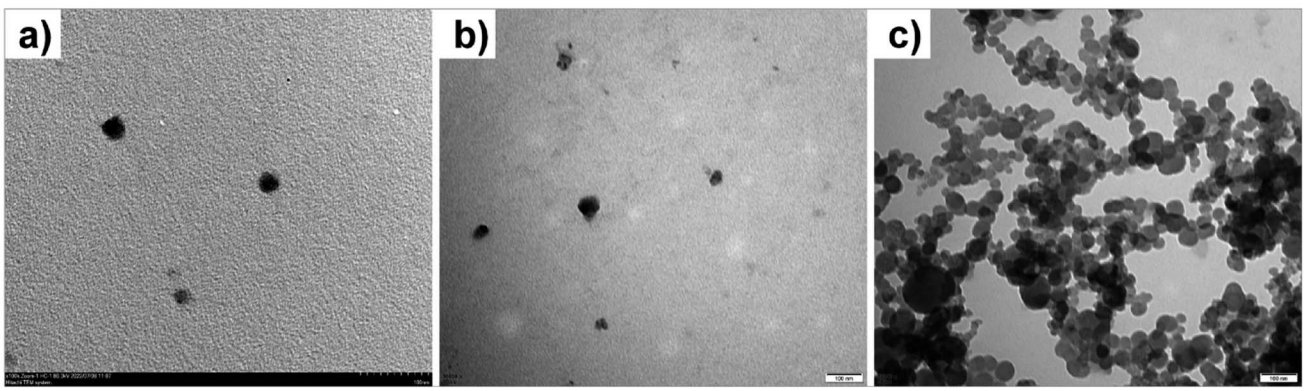

Fig. 4 TEM micrographs of (a) only Pb^{2+}, and PDA–EDEA–TAA liposomes: (b) before and (c) after addition of 100 μM Pb^{2+}. Scale bar is 100 nm.

2.3 Detection of Pb^{2+} using PDA–EDEA–TAA (or PDA–EDEA–OA) liposomes in aqueous solution

After obtaining the optimal detection system, we then evaluated the optical spectral changes of PDA–EDEA–TAA (or PDA–EDEA–OA) liposomes in the presence of different concentrations of Pb^{2+} (0–100 μM) at a given concentration (100 μM). As displayed in Fig. 5a and S7a,† the addition of increasing amount of Pb^{2+} resulted in a dramatically decrease of absorption intensity at 640 nm, accompanied by a simultaneous increase of a new absorption band at 550 nm, indicating this system demonstrated a typical blue-to-red transition of the PDA sensors. Notably, when the concentration of Pb^{2+} was greater than 50 μM, PDA liposomes showed a slight color transition and only a negligible absorbance change was observed, suggesting that the binding sites on the surface of PDA liposomes were saturated by the formation of Pb^{2+} complexes. In addition, the color response was quite fast, the CR value reached, approximately, 36.4% within 2 min, and the color obviously changed which could be easily observed *via* naked-eye. As the time increased, the CR value increased, gaining its maximum within 25 min (Fig. S6†). The linear relationships were observed between CR values and the concentration of Pb^{2+} in the range of 0 to 20 μM, with $R^2 = 0.9933$ and $R^2 = 0.9929$ (Fig. 5b and S7b, inset†). The maximal CR values (~63% or ~50%) were gained after adding 50 μM of Pb^{2+}, and the CR values almost remained constant when the concentration of Pb^{2+} was over 50 μM (Fig. 5b and S7b†). These results are consistent with the observation of color and spectral changes mentioned above, which further indicated the saturation of PDA–EDEA–TAA (or PDA–EDEA–OA) liposomes by Pb^{2+}. The detection of Pb^{2+} using the PDA–EDEA–TAA (or PDA–EDEA–OA) liposomes was also evaluated by fluorescence spectroscopy as the blue-to-red transition of PDA is usually accompanied by fluorescence enhancement. As expected, the fluorescence intensity was gradually increased as the concentration of Pb^{2+} increased (Fig. 5c or S7c†). A linear correlation ($R^2 =$ 0.9935 or 0.9923) was also obtained with the concentration of Pb^{2+} in the range of 0 to 20 μM (Fig. 5d and S7d, inset†). By monitoring the emission change with different concentrations of Pb^{2+} using 100 μM blue PADs, the calculated detection limits were 38 nM (PDA–EDEA–TAA) and 25 nM (PDA–EDEA–OA), respectively.

2.4 Selectivity of PDA–EDEA–TAA (or PDA–EDEA–OA) liposomes

To investigate the selectivity of PDA–EDEA–TAA and PDA–EDEA–OA liposomes for Pb^{2+}, other metal ions including Na^+, K^+, Mg^{2+},

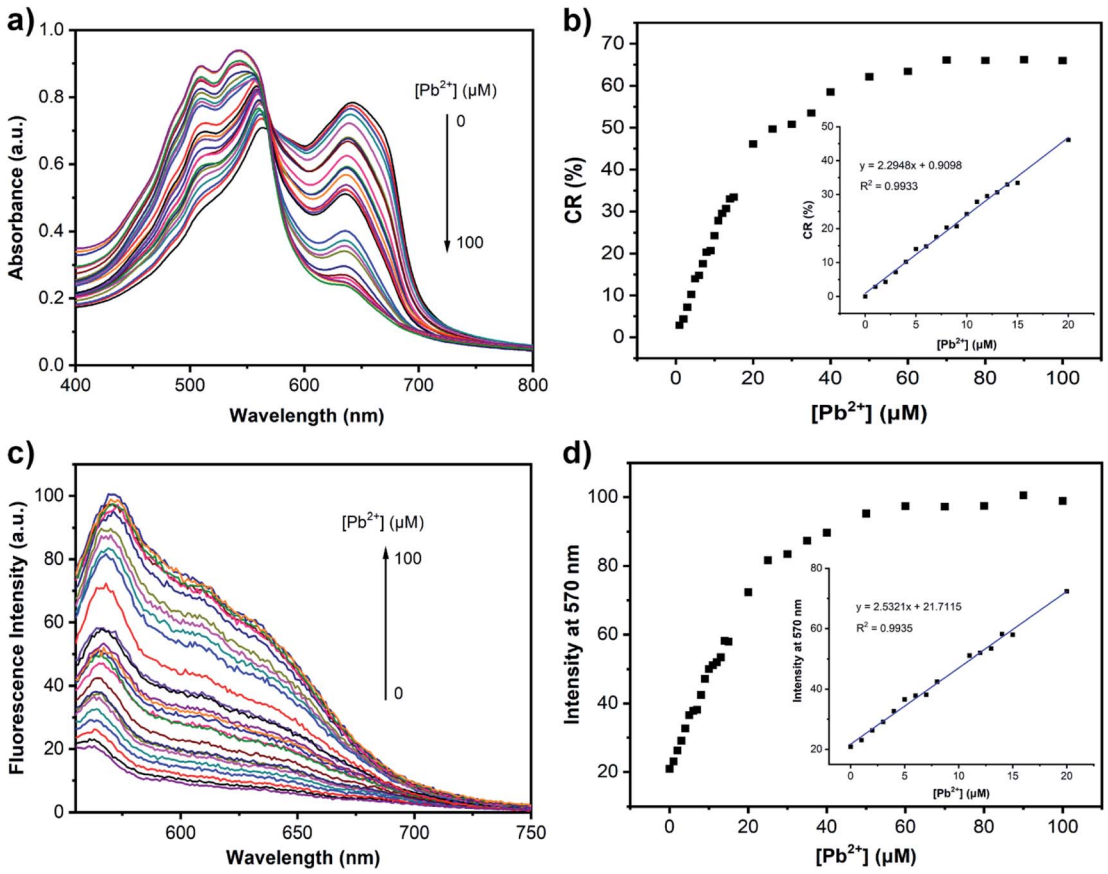

Fig. 5 (a) UV-vis absorption spectra and (b) related CR (%) values of PDA–EDEA–TAA liposomes (100 μM) in HEPES buffer (10 mM, pH = 7.4) with the increasing concentration of Pb^{2+} ions (0–100 μM) at room temperature. Inset: the linear relationship between the CR (%) value of PDA–EDEA–TAA liposomes and Pb^{2+} concentrations. (c) Fluorescence emission spectra and (d) related fluorescence intensity changes at 570 nm of PDA–EDEA–TAA liposomes (100 μM) in HEPES buffer (10 mM, pH = 7.4) upon the addition of different concentrations of Pb^{2+} ions (0–100 μM) at room temperature. Inset: the linear relationship between the fluorescence intensity of PDA–EDEA–TAA liposomes and Pb^{2+} concentrations.

Al^{3+}, Ag^{+}, Cu^{2+}, Ba^{2+}, Co^{2+}, Cr^{3+}, Fe^{3+}, Hg^{2+}, Ca^{2+}, Zn^{2+}, Cd^{2+} and Mn^{2+} were chosen to introduce into the PDA–EDEA–TAA or PDA–EDEA–OA liposomes. The UV-vis absorption spectra and corresponding color changes in the presence of various metal ions (100 μM) were distinctly shown in Fig. 6a, c, S8a and c.† It can be seen that only Pb^{2+}could cause a significant spectral change accompanied by an obvious color change. Other metal ions almost caused no spectral and color changes in PDA–EDEA–TAA or PDA–EDEA–OA liposomes. It is worth noting that PDA–EDEA–TAA and PDA–EDEA–OA liposomes showed slight color and spectral changes in the presence of Hg^{2+} and Cd^{2+}, respectively. However, the color responses of Hg^{2+} and Cd^{2+} were quite mild compared with Pb^{2+}. As control experiments, we also studied the color changes of the PDA liposomes prepared from pure PCDA to these metal ions. However, no significant color changes were observed (Fig. 7c and S9c†). Such observations indicate that the excellent selectivity of PDA–EDEA–TAA or PDA–EDEA–OA liposomes for Pb^{2+} may be plausibly ascribed to the strong interactions of Pb^{2+} with the thymine-1-acetic acid (or orotic acid) and the carboxylate carbonyl groups of the adjacent PCDA-acid moiety. The addition of Pb^{2+} might disturb the backbone of the PDA polymer, allowing the release of the strain energy imposed on the alkyl side chains generated during polymerization. The release of the side chain strain might cause partial distortion of the arrayed p-orbitals, which can lead to the observed change in optical properties.[47] To further verify the selectivities of PDA–EDEA–TAA or PDA–EDEA–OA liposomes for Pb^{2+}, interference experiments were also performed by adding Pb^{2+} into these metal ion-containing solutions and their CR values were calculated (Fig. 7b and S9b†). Relatively low CR values (0–8%) were obtained in the presence of other metal ions. However, the CR values of the mixed suspensions were enhanced after the addition of Pb^{2+} with a clear color change from blue to red. In addition, the selectivity was expressed quantitatively by the selectivity coefficient, as shown in Table S2.† The selectivity coefficient was the ratio of the slope of given metal ions to the slope of Pb^{2+}, and the selectivity coefficients were found in the range of 0.3–15%. These results indicate that the presented PDA–EDEA–TAA and PDA–EDEA–OA liposomes could act as sensitive and selective colorimetric sensors to detect Pb^{2+} with no or little interference from other competitive metal ions.

2.5 Determination of Pb^{2+} content in actual water samples

To further investigate the applicability of the probes, PDA–EDEA–TAA and PDA–EDEA–OA were used to detect Pb^{2+} in real samples. The water samples were collected from a tap in the laboratory at Northwest A&F University. They were used without further purification after sitting for 12 h and were divided into two groups. The recovery experiments were conducted by standard addition methods. All real samples were first spiked with different concentrations of Pb^{2+}, and then precisely detected with the probe PDA–EDEA–TAA or PDA–EDEA–OA (100 μM). As the obtained results listed in Table 1, the recoveries for the method were found in the range of 101.3–103.6%, with the

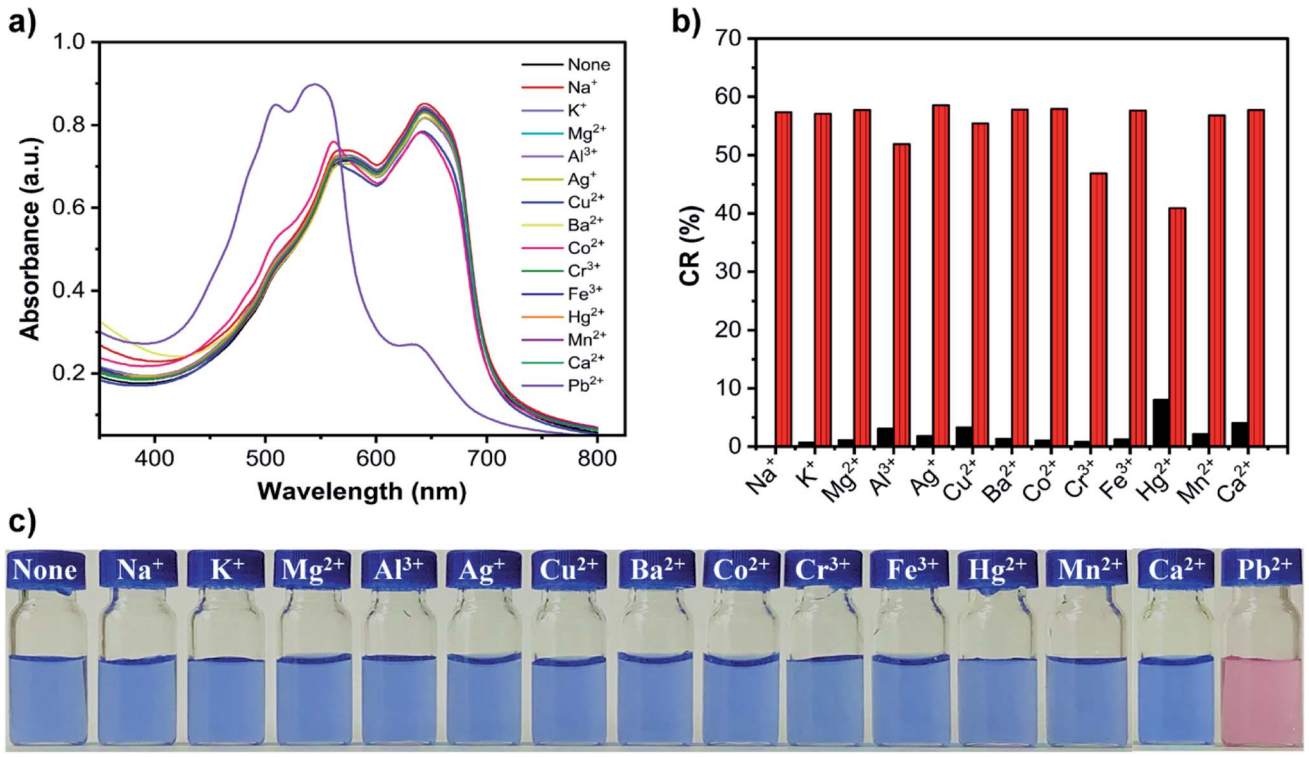

Fig. 6 (a) UV-vis absorption spectra and (b) related CR (%) values of PDA–EDEA–TAA liposomes in the presence of different metal ions. Black bars represent the CR (%) values after the addition of the given metal ions (100 μM). Red bars represent the CR (%) values after the addition of Pb^{2+} ions (100 μM) to the respective solution. (c) The color changes of PDA–EDEA–TAA liposomes (100 μM) upon the addition of different metal ions in HEPES buffer (10 mM, pH = 7.4) at room temperature.

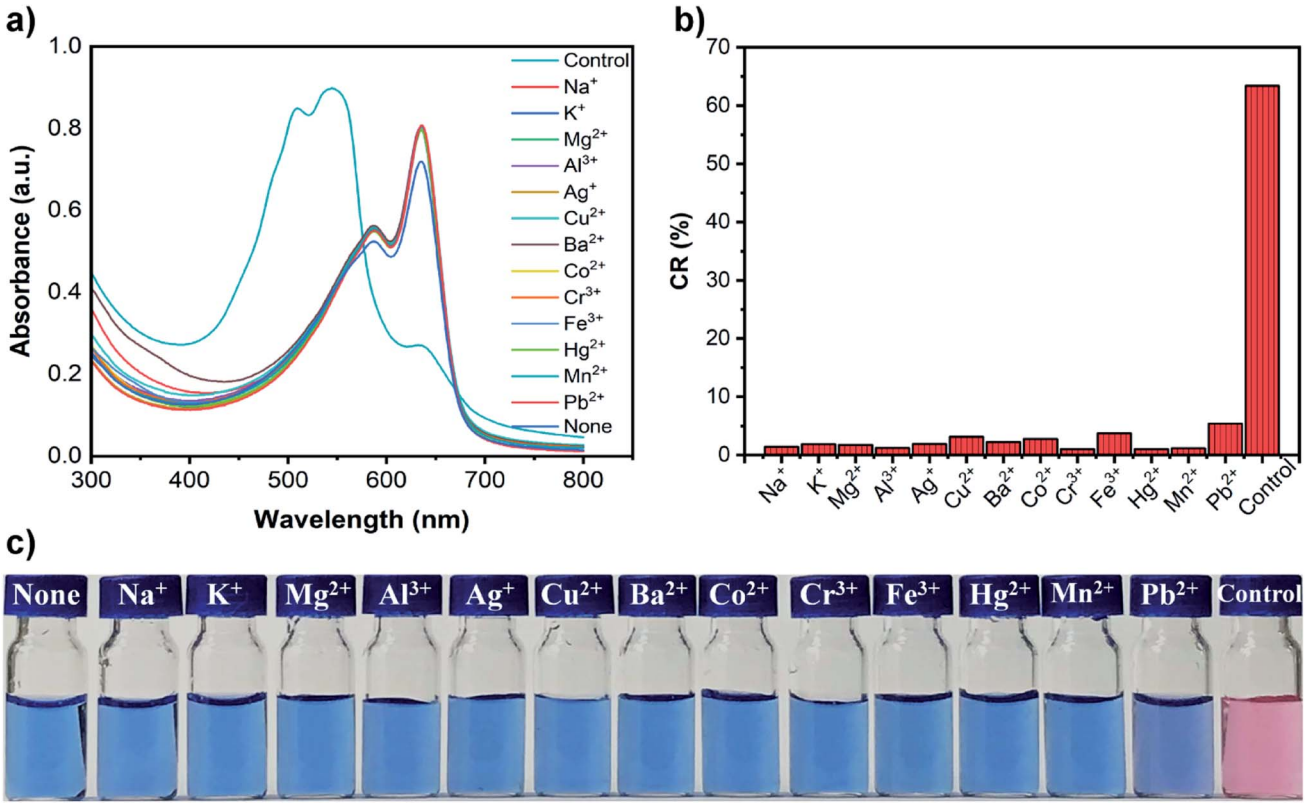

Fig. 7 (a) UV-vis spectra and (b) related CR (%) values of PDA liposomes prepared from pure PCDA in HEPES (10 mM, pH = 7.4) in the presence of different metal ions (100 μM) in HEPES buffer (10 mM, pH = 7.4) at room temperature. (c) Corresponding color changes of PDA liposomes prepared from pure PCDA after adding different metal ions. Control group was set as the CR (%) value and color change of PDA–EDEA–TAA liposomes in the presence of Pb^{2+} (100 μM).

Table 1 Application of PDA liposomes in detection of Pb^{2+} in water samples

PDA liposome	Added (μM)	Detected ($\bar{x}^1$ ± RSD^2) (μM)	Recovery (%)	Relative error (%)
PDA–EDEA–TAA	0	0	—	—
	5.0	5.13 ± 0.03	102.6	2.6
	10.0	10.21 ± 0.03	102.1	2.1
PDA–EDEA–OA	0	0	—	—
	5.0	5.18 ± 0.03	103.6	3.6
	10.0	10.13 ± 0.02	101.3	1.3

relative standard deviations (RSD) ranging from 2% to 3% and the relative errors being of 1.3% to 3.6%, a good agreement was obtained between the added and measured of spiked samples, revealing no influence of tape water matrix on the sensitivity of the Pb^{2+} analysis.

3 Conclusions

In summary, we have developed two new efficient PDA-based chemosensor systems for the detection of Pb^{2+} in aqueous solution. Among the various metal ions, PDA–EDEA–TAA and PDA–EDEA–OA displayed a selective colorimetric change from blue to red, as well as fluorescence enhancement. Most importantly, a clear color change could be easily observed *via* naked-eye in the presence of 20 μM Pb^{2+}. The detection limits of PDA–EDEA–TAA and PDA–EDEA–OA systems are 38 nM and 25 nM, respectively. Importantly, the two probes were used to trace amounts of Pb^{2+} in real water samples with good recoveries and less the relative standard deviations, indicating that the developed method had a good sensitivity and precision in real tape water matrix and can be further used for the analysis of trace Pb^{2+} in practical samples.

4 Experimental

4.1 Chemicals and instrumentation

The chemicals and instrumentation used in this study can be found in the ESI.†

4.2 Synthesis of PCDA derivatives PCDA–EDEA–TAA and PCDA–EDEA–OA

The diacetylene monomers PCDA–EDEA–TAA and PCDA–EDEA–OA were synthesized through a typical procedure as shown in Scheme S1.† 10,12-Pentacosadiynoic acid (PCDA) was reacted with *N*-hydroxysuccinimide (NHS) in the presence of 1-(3-dimethylaminopropyl)-3-ethylcarbodiimide hydrochloride (EDC·HCl), followed by reaction with 2,2′-(ethylenedioxy)bis(ethylamine) (EDEA) in anhydrous CH_2Cl_2 at room temperature, afforded PCDA derivative PCDA–EDEA with 78.4% yield. Then, PCDA–EDEA was reacted with thymine-1-acetic acid (TAA) or orotic acid (OA) in the presence of EDC·HCl and NHS in the solvent of *N*,*N*-dimethylformamide (DMF) respectively, to give the desired diacetylene monomers PCDA–EDEA–TAA and PCDA–EDEA–OA as white solids. Experimental details and characterization are provided in the ESI.†

4.3 Preparation of PDA liposomes

The PDA liposomes used in this study were achieved following the probe sonication method.[35] In short, a mixture of PCDA–EDEA–TAA (or PCDA–EDEA–OA) and PCDA with different mole ratios (5 : 5, 4 : 6, 3 : 7, 2 : 8, 1 : 9, 0 : 10) was dissolved in 1 mL of chloroform. Then, the organic solvent was completely removed under nitrogen gas and an appropriate amount of ultrapurified water was subsequently added to give a total lipid concentration of 1 mM. The resulting mixture was sonicated for 30 min at 80 °C to afford a transparent or translucent solution. The formed liposome solution was cooled and stored at 4 °C at least 6 h. The composite vesicles were converted into a deep-blue solution upon UV irradiation for 15–20 min at room temperature. The obtained PDA liposome solutions could be stored at 4 °C for one week without forming a precipitation. Pure polymerized PCDA (PDA) vesicles were prepared following a similar process.

4.4 Characterization of PDA liposomes

The morphology of PDA liposomes prepared from PCDA–EDEA–TAA and PCDA (mole ratio, 1 : 9) before or after the addition of 100 μM Pb^{2+} was characterized by using a transmission electron microscope (TEM). For the typical experiment, a drop of the freshly prepared sample was dropped onto a carbon-supported copper grid and dried gradually at room temperature before observation. Dynamic light scattering (DLS) particle size distribution of PCDA–EDEA–TAA liposomes in HEPHS before and after UV irradiation, or in the presence of 100 μM of Pb^{2+} was determined with a Zetasizer Nano ZS (Malvern Instruments Co, UK). The liposome solutions were measured at room temperature and each diameter value was an average result of continuous measurements in a 5 min period. At least, three measurements were performed for each solution. The particle size distribution was related to the scattered light intensity.[57]

4.5 Detection of Pb^{2+} using PDA liposomes

The typical experiment of Pb^{2+} detection was according to our previous method.[58] To evaluate the color change of the PDA liposomes, the colorimetric response (CR, %) was employed to determine the extent of color transition.[36,51,52] The formula is defined as follows:

$$CR = [(PB_0 - PB_1)/PB_0] \times 100\%$$

where $PB = A_{blue}/(A_{blue} + A_{red})$. A_{blue} and A_{red} represent the absorbance either at the "blue" component in the UV-vis spectrum (640 nm) or at the "red" component (550 nm). PB_0 is the ratio of the absorbance at 640 nm to that at 550 nm in the absence of Pb^{2+}, while PB_1 is the ratio of the absorbance at 640 nm to that at 550 nm after addition of different concentrations of Pb^{2+}.

4.6 Detection of Pb^{2+} in real samples

The real samples were collected from the tap in the laboratory at Northwest A&F University, Yangling, Shaanxi. They were used without further purification after sitting for 12 h and were divided into two groups. One group was pretreated with different concentrations of Pb^{2+} as the experiment group (spiked) and the other group, without any pretreatment, was the control (unspiked). The method of processing samples follows references.[59,60]

Author contributions

Shu-Wei Chen: conceptualization, supervision, methodology, investigation, writing-review & editing. Xipeng Chen: methodology, investigation, data curation. Yang Li: methodology, investigation, data curation. Yalin Yang: methodology, investigation. Yuchuan Dong: methodology. Jinwen Guo: investigation. Jinyi Wang: conceptualization, supervision, writing-review & editing.

Conflicts of interest

There are no conflicts to declare.

Acknowledgements

We gratefully acknowledge National Natural Science Foundation of China (21202131, 21874108 and 21675126), Natural Science Foundation of Shaanxi Province (2019JM-022) and the Chinese Universities Scientific Fund (2452018160, 2452021164). We thank the Life Science Research Core Services, NWAFU (Lei Chen) for technical support.

Notes and references

1 H. Needleman, *Annu. Rev. Med.*, 2004, **55**, 209–222.
2 H. L. Needleman, *Human lead exposure*, CRC Press, Boca Raton, FL, 1992, pp. 23–43.
3 Y. Finkelstein, M. E. Markowitz and J. F. Rosen, *Brain Res. Rev.*, 1998, **27**, 168–176.
4 *Guidelines for Drinking-water Quality*, World Health Organization, Geneva, Switzerland, 4th edn, 2011, p. 383.

5 P. J. Parsons, H. Qiao, K. M. Aldous, E. Mills and W. Slavin, *Spectrochim. Acta, Part B*, 1995, **50**, 1475–1480.
6 A. T. Townsend, K. A. Miller, S. McLean and S. Aldous, *J. Anal. At. Spectrom.*, 1998, **13**, 1213–1219.
7 X. Jia, J. Li and E. Wang, *Electroanalysis*, 2010, **22**, 1682–1687.
8 H. N. Kim, W. X. Ren, J. S. Kim and J. Yoon, *Chem. Soc. Rev.*, 2012, **41**, 3210–3244.
9 J. Li and Y. Lu, *J. Am. Chem. Soc.*, 2000, **122**, 10466–10467.
10 J. Liu and Y. Lu, *J. Am. Chem. Soc.*, 2003, **125**, 6642–6643.
11 Y. Xiang, A. Tong and Y. Lu, *J. Am. Chem. Soc.*, 2009, **131**, 15352–15357.
12 T. Li, E. Wang and S. Dong, *Anal. Chem.*, 2010, **82**, 1515–1520.
13 X.-H. Zhao, R.-M. Kong, X.-B. Zhang, H.-M. Meng, W.-N. Liu, W. Tan, G.-L. Shen and R.-Q. Yu, *Anal. Chem.*, 2011, **83**, 5062–5066.
14 P. Chen, B. Greenberg, S. Taghavi, C. Romano, D. van der Lelie and C. He, *Angew. Chem.*, 2005, **117**, 2775–2779.
15 I.-B. Kim, A. Dunkhorst, J. Gilbert and U. H. F. Bunz, *Macromolecules*, 2005, **38**, 4560–4562.
16 Z. Wang, J. H. Lee and Y. Lu, *Adv. Mater.*, 2008, **20**, 3263–3267.
17 H. Y. Lee, D. R. Bae, J. C. Park, H. Song, W. S. Han and J. H. Jung, *Angew. Chem.*, 2009, **121**, 1265–1269.
18 L. Beqa, A. K. Singh, S. A. Khan, D. Senapati, S. R. Arumugam and P. C. Ray, *ACS Appl. Mater. Interfaces*, 2011, **3**, 668–673.
19 S. Rouhani and S. Haghgoo, *Sens. Actuators, B*, 2015, **209**, 957–965.
20 S. Deo and H. A. Godwin, *J. Am. Chem. Soc.*, 2000, **122**, 174–175.
21 J. Y. Kwon, Y. J. Jang, Y. J. Lee, K. M. Kim, M. S. Seo, W. Nam and J. Yoon, *J. Am. Chem. Soc.*, 2005, **127**, 10107–10111.
22 Q. He, E. W. Miller, A. P. Wong and C. J. Chang, *J. Am. Chem. Soc.*, 2006, **128**, 9316–9317.
23 L. Marbella, B. Serli-Mitasev and P. Basu, *Angew. Chem., Int. Ed.*, 2009, **48**, 3996–3998.
24 X. Pan, Y. Wang, H. Jiang, G. Zou and Q. Zhang, *J. Mater. Chem.*, 2011, **21**, 3604–3610.
25 M. A. Reppy and B. A. Pindzola, *Chem. Commun.*, 2007, 4317–4338.
26 X. Sun, T. Chen, S. Huang, L. Li and H. Peng, *Chem. Soc. Rev.*, 2010, **39**, 4244–4257.
27 B. Yoon, S. Lee and J.-M. Kim, *Chem. Soc. Rev.*, 2009, **38**, 1958–1968.
28 X. Chen, G. Zhou, X. Peng and J. Yoon, *Chem. Soc. Rev.*, 2012, **41**, 4610–4630.
29 A. Reichert, J. O. Nagy, W. Spevak and D. Charych, *J. Am. Chem. Soc.*, 1995, **117**, 829–830.
30 Y. K. Jung and H. G. Park, *Biosens. Bioelectron.*, 2015, **72**, 127–132.
31 S. Y. Okada, R. Jelinek and D. Charych, *Angew. Chem., Int. Ed.*, 1999, **38**, 655–659.
32 S. Kolusheva, T. Shahal and R. Jelinek, *J. Am. Chem. Soc.*, 2000, **122**, 776–780.
33 D.-E. Wang, J. Yan, J. Jiang, X. Liu, C. Chang, J. Xu, M.-S. Yuan, X. Han and J. Wang, *Nanoscale*, 2018, **10**, 4570–4578.
34 G. Zhou, F. Wang, H. Wang, S. Kambam, X. Chen and J. Yoon, *ACS Appl. Mater. Interfaces*, 2013, **5**, 3275–3280.
35 D.-E. Wang, Y. Zhang, T. Li, Q. Tu and J. Wang, *RSC Adv.*, 2014, **4**, 16820–16823.
36 S. Kolusheva, R. Zadmard, T. Schrader and R. Jelinek, *J. Am. Chem. Soc.*, 2006, **128**, 13592–13598.
37 Y. K. Jung, T. W. Kim, H. G. Park and H. T. Soh, *Adv. Funct. Mater.*, 2010, **20**, 3092–3097.
38 J. Lee, H.-J. Kim and J. Kim, *J. Am. Chem. Soc.*, 2008, **130**, 5010–5011.
39 D. A. Jose, S. Stadlbauer and B. König, *Chem.–Eur. J.*, 2009, **15**, 7404–7412.
40 D. A. Jose and B. König, *Org. Biomol. Chem.*, 2010, **8**, 655–662.
41 K. M. Kim, D. J. Oh and K. H. Ahn, *Chem.–Asian J.*, 2011, **6**, 122–127.
42 X. Chen, J. Lee, M. J. Jou, J.-M. Kim and J. Yoon, *Chem. Commun.*, 2009, 3434–3436.
43 X. Chen, S. Kang, M. J. Kim, J. Kim, Y. S. Kim, H. Kim, B. Chi, S.-J. Kim, J. Y. Lee and J. Yoon, *Angew. Chem., Int. Ed.*, 2010, **49**, 1422–1425.
44 D.-E. Wang, L. Zhao, M.-S. Yuan, S.-W. Chen, T. Li and J. Wang, *ACS Appl. Mater. Interfaces*, 2016, **8**, 28231–28240.
45 J. Yoon, S. K. Chae and J.-M. Kim, *J. Am. Chem. Soc.*, 2007, **129**, 3038–3039.
46 J. Lee, H. T. Chang, H. An, S. Ahn, J. Shim and J.-M. Kim, *Nat. Commun.*, 2013, **4**, 2461.
47 K. M. Lee, X. Chen, W. Fang, J.-M. Kim and J. Yoon, *Macromol. Rapid Commun.*, 2011, **32**, 497–500.
48 S. Zhang, B. Shi and G. Yang, *Macromol. Res.*, 2020, **28**, 51–56.
49 P. Narkwiboonwong, G. Tumcharern, A. Potisatityuenyong, S. Wacharasindhu and M. Sukwattanasinitt, *Talanta*, 2011, **83**, 872–878.
50 D. H. Kang, H.-S. Jung, N. Ahn, S. M. Yang, S. Seo, K.-Y. Suh, P.-S. Chang, N. L. Jeon, J. Kim and K. Kim, *ACS Appl. Mater. Interfaces*, 2014, **6**, 10631–10637.
51 Y. Li, L. Wang, X. Yin, B. Ding, G. Sun, T. Ke, J. Chen and J. Yu, *J. Mater. Chem. A*, 2014, **2**, 18304–18312.
52 M. Wang, F. Wang, Y. Wang, W. Zhang and X. Chen, *Dyes Pigm.*, 2015, **120**, 307–313.
53 G. Yang, Z. Nie, S. Zhang, Z. Ge, J. Zhao, J. Zhang and B. Li, *Macromol. Res.*, 2020, **28**, 1192–1197.
54 H. Yin and S.-X. Liu, *Inorg. Chem. Commun.*, 2009, **12**, 187–190.
55 X. Y. Liu, D. R. Bai and S. Wang, *Angew. Chem., Int. Ed.*, 2006, **45**, 5475–5478.
56 M.-S. Yuan, Z.-Q. Liu and Q. Fang, *J. Org. Chem.*, 2007, **72**, 7915–7922.
57 Y.-S. Cho and K. H. Ahn, *J. Mater. Chem. B*, 2013, **1**, 1182–1189.
58 D.-E. Wang, Y. Wang, C. Tian, L. Zhang, X. Han, Q. Tu, M. Yuan, S. Chen and J. Wang, *J. Mater. Chem. A*, 2015, **3**, 21690–21698.
59 L. Lan, Q. Niu and T. Li, *Anal. Chim. Acta*, 2018, **1023**, 105–114.
60 Y. Zhang, L. Chen, J. Yang, Y. Zhang and M.-S. Yuan, *Spectrochim. Acta, Part A*, 2020, **232**, 118163.